


Article

High-Quality Syngas Production by Chemical Looping Gasification of Bituminite Based on NiFe₂O₄ Oxygen Carrier

Ming Yang ¹, Da Song ^{1,2} , Yang Li ³, Jinzeng Cao ², Guoqiang Wei ^{2,*} and Fang He ^{1,*}¹ College of Chemistry and Bioengineering, Guilin University of Technology, Guilin 541004, China² Institute of Biomass Engineering, Key Laboratory of Energy Plants Resource and Utilization, Ministry of Agriculture and Rural Affairs, South China Agricultural University, Guangzhou 510642, China³ College of Chemistry and Engineering, Northeast Petroleum University, Daqing 163318, China

* Correspondence: weigq@scau.edu.cn (G.W.); hefang@glut.edu.cn (F.H.)

Abstract: Chemical looping gasification (CLG) is an effective coal utilization technology. In this work, the CLG of bituminite was investigated through fixed-bed batch experiments using NiFe₂O₄ oxygen carrier (OC) to achieve high-quality syngas. The changes in the phase of the oxygen carrier during the chemical looping reaction and the reaction mechanism were explored. The results show that elevated temperature and adding a fraction of steam facilitate the gasification reaction. Adding an appropriate amount of ZrO₂ into the NiFe₂O₄ and modification with alkali metal can enhance the performance of the oxygen carrier. A carbon conversion of 95% and a syngas (CO and H₂) selectivity of 86% were obtained under the optimized reaction conditions of 950 °C, an oxygen-carrier-to-bituminite (O/B) ratio of 7:3, a NiFe₂O₄/ZrO₂ ratio of 7:3, and a steam rate of 0.08 mL/min. Modification of the NiFe₂O₄ by doping alkali metal can significantly facilitate the CLG process. Alkali lignin ash has a more pronounced modifying effect on oxygen carriers than K₂CO₃. The NiFe₂O₄ OC underwent a gradual reduction in Ni²⁺ → Ni and Fe³⁺ → Fe^{8/3+} → Fe²⁺ → Fe processes during the gasification reaction phase. In addition, 20 redox cycles were conducted to demonstrate the oxygen carriers' good cyclic reaction performance in the CLG process. After 20 redox cycles, the carbon conversion rate was maintained at about 90%, and the syngas selectivity was stably kept at over 80%. This work laid the theoretical foundation for the clean and efficient use of bituminite.



check for updates

Citation: Yang, M.; Song, D.; Li, Y.; Cao, J.; Wei, G.; He, F. High-Quality Syngas Production by Chemical Looping Gasification of Bituminite Based on NiFe₂O₄ Oxygen Carrier. *Energies* **2023**, *16*, 3385. <https://doi.org/10.3390/en16083385>

Academic Editor: Vladislav A. Sadykov

Received: 2 March 2023

Revised: 3 April 2023

Accepted: 3 April 2023

Published: 12 April 2023



Copyright: © 2023 by the authors. Licensee MDPI, Basel, Switzerland. This article is an open access article distributed under the terms and conditions of the Creative Commons Attribution (CC BY) license (<https://creativecommons.org/licenses/by/4.0/>).

Keywords: chemical looping gasification (CLG); bituminite; NiFe₂O₄; syngas; oxygen carrier; alkali metal

1. Introduction

The use of coal has always played an important role in the development of mankind. Coal has a wide range of applications in all industries. In 2020, global coal production was 7.742 billion tonnes, and consumption was 15.14 EJ. Fossil fuels (coal is estimated at around 60%) make up a major part of the world energy market and still dominate the current world energy [1,2]. Using coal as the fuel and chemical industry raw material guarantees its essential role in energy. Although the massive conventional utilization of coal brings economic benefits, it also generates large amounts of harmful gases such as CO₂ and SO₂, which aggravate global warming and cause significant environmental damage. In addition, the problem of the low conversion rate of traditional coal utilization is also a great challenge. Therefore, there is an urgent need to find a new coal utilization method to realize the efficient and clean utilization of coal [3,4].

Chemical looping combustion technology (CLC) was first proposed in 1983 [5], which has achieved a series of research advances [6–8]. Chemical looping gasification technology (CLG) [9–11] was an extension of chemical looping combustion technology. The difference between CLG technology and traditional gasification technology mainly lies in consuming lattice oxygen in oxygen carriers instead of traditional molecular oxygen. The principle of the CLG reaction is shown in Figure 1. In the fuel reactor, the solid fuel reacts with OC, and

the OC is reduced. In the air reactor, the reduced oxygen carrier is reoxidized to its initial state by air. Along with the circulation of the oxygen carrier between the two reactors, the coal is continuously converted into high-quality syngas. The main components of the syngas are CO, CO₂, H₂, and CH₄. The syngas can be used as clean fuels and raw materials to synthesize value-added chemicals. CLG technology has the advantages of a cheap oxygen source, low energy consumption, production with high heat value, good selectivity, avoiding dilution of products by an inert gas, and effective regulation of pollutants, etc. Moreover, the syngas produced by chemical looping gasification can produce a series of high-value chemical products such as ethanol, gasoline, and ethylene. Therefore, the improvement and optimization of coal gasification technology can not only increase economic efficiency but also improve the efficiency of utilization and significantly reduce environmental pollution. Therefore, CLG technology has an extensive application prospect and fits well with the current popular policy of carbon peaking and carbon neutrality.

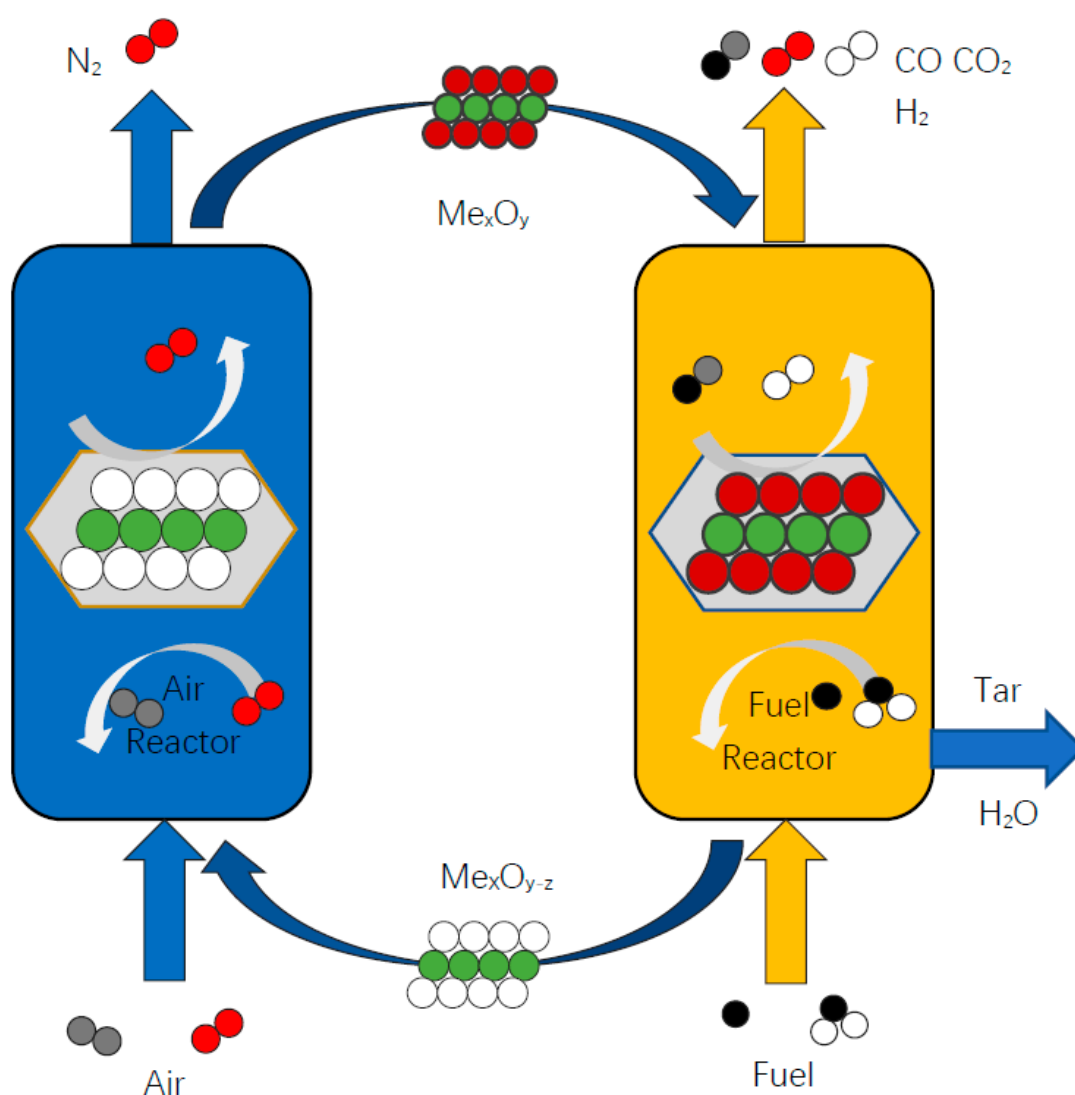


Figure 1. Schematic diagram of the CLG principle.

For CLG technology, the main research work nowadays focuses on the screening and preparation process of oxygen carriers, the design of reactors [12–14], the regulation of reaction conditions, the experiments in the reaction system, and the system analysis [15,16]. Among them, the screening of OCs plays a key role in the whole work. So far, the main types of oxygen carriers found are single-component metal oxygen carriers, composite metal oxy-

gen carriers, and nonmetal oxygen carriers. Current research on oxygen carriers is focused on: Fe-based [17–19], Ni-based [20–22], Cu-based [23–25], Co-based, Mn-based [26,27], etc. Nonmetal oxides mainly focus on CaSO₄ [28–30]. Most single-component oxygen carriers have certain limitations. For example, Fe-based OCs have low prices, high melting points, and excellent theoretical oxygen loading rates. However, the utilization of Fe-based OCs is limited due to their weak oxygen transfer ability and thermodynamic limitation. Wei and co-workers [31] demonstrated that CLG of lignite with hematite as an OC could obtain high-quality syngas. However, Fe-based OCs exhibited a low redox reaction rate with coal, especially coal char. Ni-based OCs have good reactivity and large oxygen loading capacity but have serious carbon accumulation and toxicity problems. Conversely, composite metal oxygen carriers have their unique advantages [32–35]. For example, the Fe–Ni composite oxygen carrier retains the high reactivity and oxygen-carrying capacity of Ni and the low cost, anti-sintering capacity, and high mechanical strength of Fe. It neutralizes the problems of carbon accumulation of Ni and poor reactivity of Fe, which is a more optimal choice. Song et al. [36] investigated the combustion characteristics of coal CLG with Fe–Ni bimetallic oxygen carriers using a 1 kWth scale serial fluidized bed reactor, and the results showed that the addition of NiO significantly improved the carbon conversion and carbon capture efficiency, which was mainly attributed to the formation of a new phase (NiFe₂O₄). Anqing Zheng et al. [37] used NiFe₂O₄ as an OC for syngas production and tar removal and achieved good experimental results. Huang et al. [38] confirmed the excellent reactivity of NiFe₂O₄ in the biomass CLG process. Zhao et al. [11] used NiFe₂O₄ and CuFe₂O₄ as oxygen carriers to gasify lignite by CLG and achieve 70% carbon conversion and 75% syngas selectivity. Reactor design is also a key factor affecting the mass and heat transfer in the chemical looping gasification process. In recent years, with the continuous development of chemical looping gasification technology, the reactors used in research have also developed from the initial thermogravimetric TGA reactors and fixed bed reactors to circulating fluidized bed industrial reactors, solid fuel chemical looping combustion devices, etc. Lyngfelt et al. [39] of Chalmers University of Technology, Sweden, designed and built the world's first continuously operating 10 kWth chemical looping combustion serial fluidized bed reactor in 2001, which contains an air reactor, fuel reactor, cyclone separator, and other units. The Guangzhou Institute of Energy Research, Chinese Academy of Sciences [40] also successfully designed and built a 10 kWth biomass chemistry looping gasification serial fluidized bed reactor.

Meanwhile, adding some inert components, such as ZrO₂, into the oxygen carrier can further improve the oxygen carrier reaction performance. Because ZrO₂ can also be used as a heat carrier to transfer and store heat, it can also improve the reaction activity of the oxygen carrier, which can further improve the performance and extend the service life of the oxygen carrier. Li et al. [41] found that Fe₂O₃ and other particles could be well dispersed on the surface of ZrO₂, and the experiment shows that the oxygen carriers loaded with ZrO₂ exhibit excellent reaction performance. Adding an appropriate amount of alkali metal can significantly facilitate the CLG process. On the one hand, alkali metal can have a catalytic effect on the pyrolysis and gasification of biomass and thus improve its utilization efficiency [42,43]. Jiang et al. [42] found that alkali metals can promote H₂ and CO formation in the study of rice straw and rice bran steam gasification. On the other hand, adding alkali metals changes the apparent structure of oxygen carriers' void properties. The preparation processes of oxygen carriers are mainly co-precipitation [44,45], mechanical mixing [24], and the impregnation method [33], which have their own advantages and disadvantages and are suitable for different reaction systems and atmospheres.

Some studies have been conducted on NiFe₂O₄ as an oxygen carrier to gasify coal. However, up to date, there is a lack of systematic evaluation of the catalytic bituminite with NiFe₂O₄ as an oxygen carrier under different reaction atmospheres. It also has been difficult to maintain high conversion and effective gas yield during long-term cycling. The oxygen carrier's physical phase and crystallographic changes during the reaction and cycling process have also been less explored. In this paper, by changing the temperature,

O/B, and adding inert components, steam, and alkali metal, the bituminite gasification process under different reactions was systematically investigated. The effect of alkali metals has been thoroughly explored. Bituminite coal can always maintain a high conversion rate in the long-term cycle. XRD, SEM, and TEM study the change law of oxygen carriers in the reaction and cycle process. After optimizing operating conditions, the technical feasibility of using NiFe_2O_4 oxygen carriers to achieve high-quality syngas via CLG from bituminite is verified and discussed.

2. Experiment and Apparatus

2.1. Materials

In this study, NiFe_2O_4 was selected as the oxygen carrier required for the reaction. The specification of NiFe_2O_4 is 30 nm spherical with a purity of more than 99.5%. The manufacturing method is mainly through the co-precipitation method. The prepared oxygen carrier has good sphericity, reaction performance, and industrialized mass production. The raw material used for the reaction was Ningxia bituminite. Elemental and industrial analyses of raw materials were carried out, as shown in Table 1. XRF analysis of bituminite was carried out, as shown in Table 2. The alkaline lignin ash used in the experiment was produced by burning alkaline lignin in a muffle furnace for 2 h at 600 °C temperature.

Table 1. Proximate and ultimate analysis of coal.

Ultimate analysis (wt%, daf)	C	H	N	S	O*	Q _{net, v, d} 26.72 KJ/g
	69.77	3.91	0.61	1.06	12.97	
Proximate analysis (wt%)	M	V	A	FC		
	10.22	40.30	11.68	37.8		

$$\text{O}^* = 100 - \text{C} - \text{H} - \text{N} - \text{S} - \text{A}.$$

Table 2. XRF analysis of bituminite.

Element	O	Ca	Na	Fe	Si	Al	Mg	S	Others
Content (%)	50.12	17.07	13.14	7.05	4.62	2.90	1.70	1.55	1.85

The results show that bituminite coal has high volatile content, high moisture, and low calorific value. Directly used for conventional combustion to convert the resource utilization efficiency is low and has environmental risks. The use of chemical looping gasification technology to obtain high-quality syngas can effectively improve the efficiency of coal resource utilization and reduce environmental pollution in the conversion process.

2.2. Experimental Section

The OC samples were characterized and analyzed by X-ray diffraction (model: X'Pert Pro MPD (PW3040/60)) manufactured by PANalytical, Netherlands. The operating conditions are as follows: Cu $K\alpha$ radiation ($\lambda = 0.15406$ nm), working voltage 40 kV, current 40 mA, scanning step $0.0167^\circ \text{ S}^{-1}$, scanning diffraction angle (2θ) $5\text{--}80^\circ$. The field emission Scanning electron microscope (SEM) made by Hitachi, Japan (S-4800) was used to characterize the micro-morphology of oxygen carriers. The operating conditions are as follows: accelerating voltage 2 kV, working distance 4 mm. To further observe the microscopic morphology and lattice spacing variation in the oxygen carriers, the transmission electron microscope (TEM) manufactured by JEOL, Japan (JEM-2100F) was used in this experiment. The instrument operates at an accelerating voltage of 200 V with a resolution of 0.14 nm and 0.19 nm for point and line, respectively. The gas chromatograph produced by Agilent, USA (Model: 7890A) was used to analyze the composition of synthetic gas products. The composition and concentration of gas products were determined by the normalization method.

The experimental setup is shown schematically in Figure 2. Before the experiment, the bituminite was dried for 24 h at 105 °C in a blast drying box. The weighed oxygen carrier and bituminite were put into the feeder of the material control unit. Argon gas was used as a protective gas and carrier gas. The rate of argon gas in the reactor is 100 mL/min, blowing 30 min to ensure that the experimental device exhausts residual air. Then turn on the temperature controller switch, and the fixed bed was heated to the temperature set by the reaction at a heating rate of 30 °C/min, turn on the feed-in switch and let the material fall. At the same time, an airbag is used to start collecting the gas after the reaction. At the end of the experiment, the temperature control switch is turned off. After the reaction, the airbag and solid product are stored for testing, and then the power switch to the experimental setup is switched off.

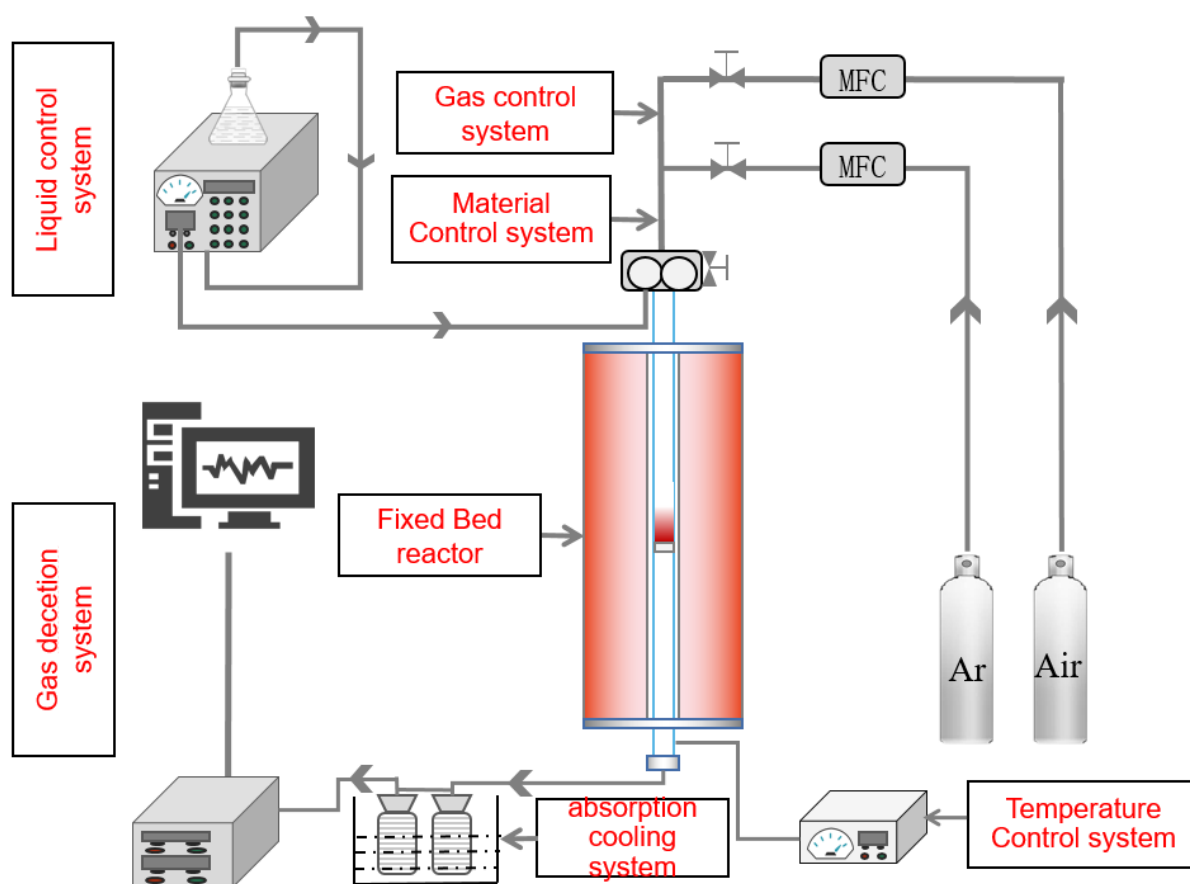


Figure 2. Schematic layout of CLG.

The raw material was 1 g of bituminite, and the amount of the rest of the material was converted according to the mass ratio mentioned. First, experiments were conducted at a temperature range of 750~1000 °C. Every 50 °C, we selected one experimental point, with an O/B ratio of 1:1. Second, different ratios of O/B of 0/1, 3/7, 4/6, 5/5, 6/4, 7/3, and 8/2 were studied at a reaction temperature of 950 °C. Third, the effect of the NiFe₂O₄-to-ZrO₂ ratio was studied at the ratio of O/B of 7:3. Then, the effect of steam and alkali metal addition on the reaction characteristics of bituminite CLG was studied at a reaction temperature of 950 °C with an oxygen-carrier-to-bituminite ratio of 7:3. Subsequently, experiments with different steam addition and long-term redox were performed under the conditions of 950 °C, oxygen-carrier-to-bituminite (O/B) ratio of 7:3, NiFe₂O₄/ZrO₂ ratio of 7:3, and steam rate of 0.08 mL/min. Each cycle was divided into a reduction phase and an air re-oxidation phase.

2.3. Data Evaluation

Calculate the parameters required for the reaction according to the following formulae:

$$\text{Carbon Conversion} = \frac{12 \times 273 \times (V_{\text{CO}} + V_{\text{CO}_2} + V_{\text{CH}_4} + nV_{\text{C}_n\text{H}_m})}{22.4 \times 303 \times m_0 \times M_c} \times 100\%$$

$$\text{Relative concentrations} = \frac{V_i}{\sum V_i} \times 100\%$$

$$\text{Syngas selectivity} = \frac{(V_{\text{CO}} + V_{\text{H}_2})}{V_{\text{C}} \times \text{HyOz}} \times 100\%$$

$$\text{Carbon balance} = \frac{12 \times (X_c + X_o)}{m_0 \times M_c} \times 100\%$$

where M_c (carbon content in coal, %); V (gas volume, L); m_0 (added coal quality, g); X_c (the amount of carbon contained in the gas phase products at the end of the gasification reaction, mol); and X_o (the amount of carbon contained in the products of combustion of unreacted carbon-containing substances, mol).

3. Results and Discussion

3.1. Effect of Temperature on CLG

The effect of temperature on the bituminite CLG is shown in Figure 3. Obviously, the temperature significantly affects the CLG. As the temperature increases, the proportion of CO in the produced gas increases, and the proportion of CO₂ and CH₄ decreases. The elevated temperature promotes the carbon thermal reaction, consuming CO₂ and producing large amounts of CO (CO₂ + C → 2CO). The decrease in CH₄ is mainly due to the cleavage of CH₄ in the high-temperature environment promoted (CH₄ → C + 2H₂). The syngas selectivity has also improved due to the increase in CO and H₂ and the decrease in CO₂. The carbon conversion increased from 15% to about 29%. This is because the pyrolysis of bituminite (Bituminite → Gas + Char + Tar) and the gasification of char and tar (Tar/Char → Gas) are both endothermic. Elevating the gasification temperature can promote a positive shift in the reaction equilibrium. The elevated temperature can also enhance the activity of the oxygen carrier, thus promoting the gasification efficiency of the oxygen carrier with pyrolysis volatiles and coke, which facilitates the oxygen carrier to better promote the gasification of bituminite. More C/H elements in the bituminite were converted from solid to gaseous products, increasing carbon conversion. However, the carbon conversion and syngas selectivity increased slowly at 1000 °C compared with 950 °C. The reaction thermodynamics reached equilibrium at 950 °C, and excessive temperature will greatly increase the system's thermal load. High temperature (>950 °C) may also lead to particle agglomeration and sintering of the OC [46,47]. Moreover, high temperature promotes the combustion reaction of the H₂ and oxygen carriers, resulting in a decrease in the proportion of the product of H₂. Overall, the experimental gasification temperature was set to 950 °C.

3.2. Effect of O/B on CLG

The effects of the oxygen-carrier-to-bituminite (O/B) ratio on the CLG performance are shown in Figure 4. When the ratio of O/B increased from 1 to 4, the carbon conversion showed an increasing trend from 18.55% to 49.63%. The OC mainly provides lattice oxygen to participate in the gasification reaction, and an increased O/B ratio will supply more lattice oxygen, thus improving the reaction performance. The bituminite reacts more completely with the oxygen carrier, increasing the conversion of volatiles and char to syngas (Me_xO_y + C → Me_xO_{y-1} + CO/Me_xO_y + Volatile → Me_xO_{y-1} + CO + H₂). It is noted that as the O/B ratio increased, the syngas selectivity decreased from 91.76% to 77.19%. The reason is mainly that with the addition of excess oxygen carriers, the product CO reacts with the excess lattice oxygen provided by the oxygen carriers and is

over-oxidized to CO_2 , resulting in a rising CO_2 content ($\text{Me}_x\text{O}_{y-1} + \text{CO} \rightarrow \text{CO}_2 + \text{Me}_x\text{O}_y$). In addition, a part of generated hydrogen in the syngas is oxidized in-depth ($\text{Me}_x\text{O}_{y-1} + \text{H}_2 \rightarrow \text{H}_2\text{O} + \text{Me}_x\text{O}_y$). As an O/B ratio of 7:3, carbon conversion and the syngas selectivity are at a high level, with maximum effective gas production. Therefore, an O/B ratio of 7:3 is chosen as the best reaction condition.

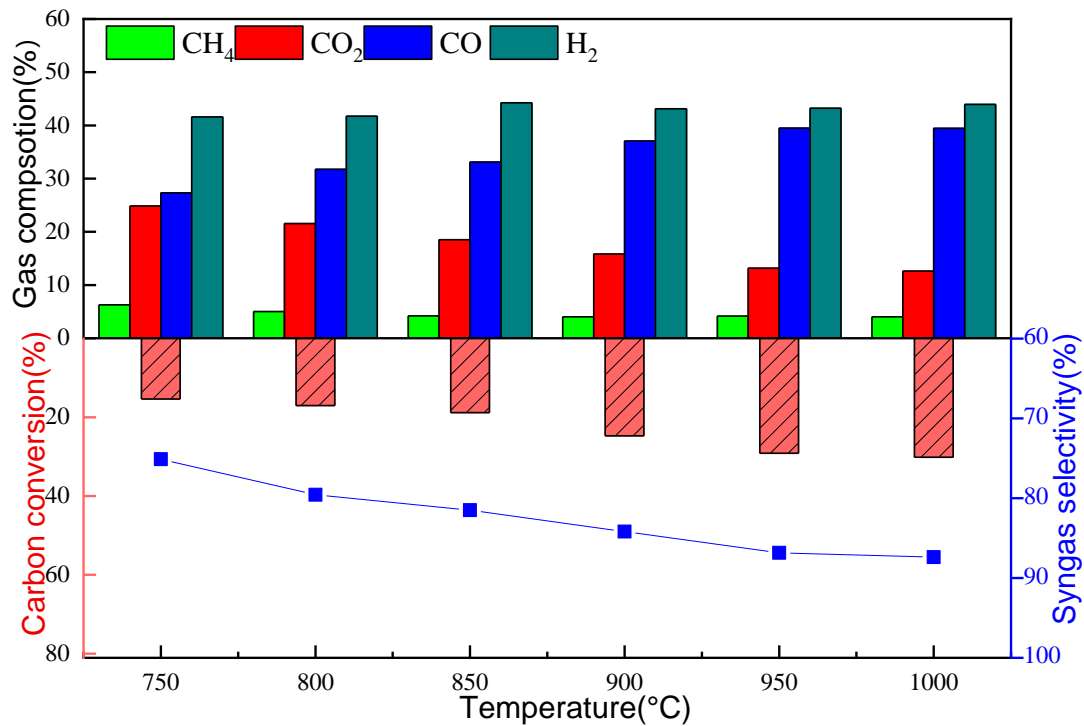


Figure 3. Effect of temperature on CLG.

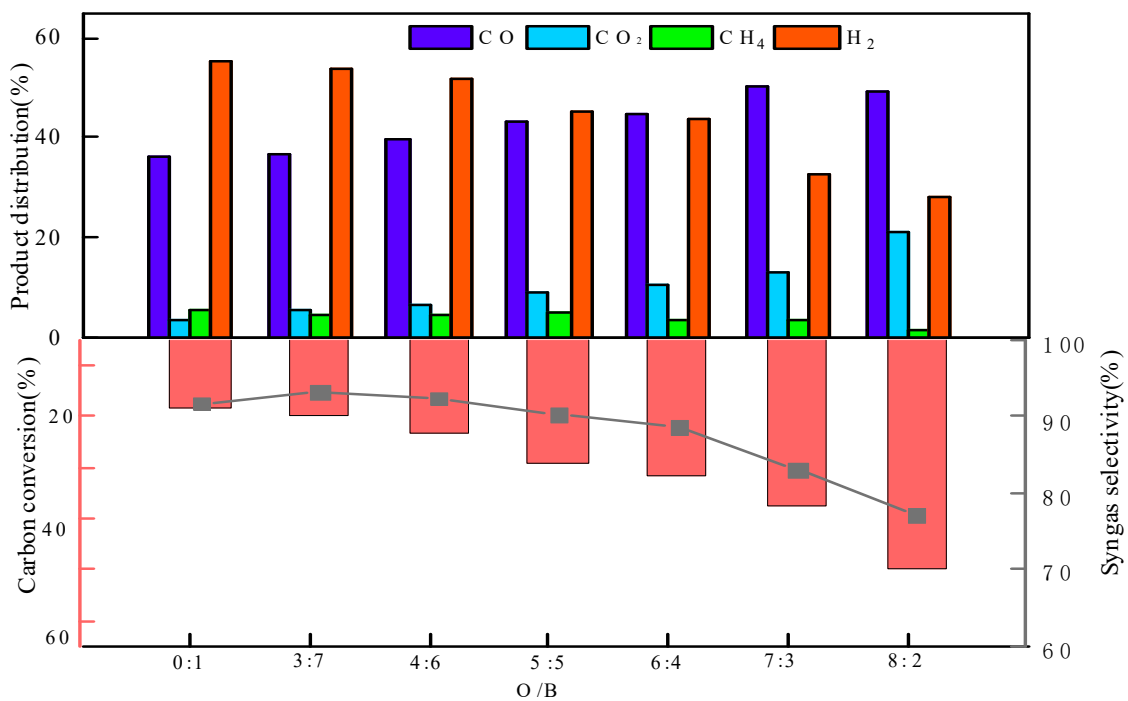


Figure 4. Effect of O/B ratio on CLG.

3.3. Effect of NiFe₂O₄-to-ZrO₂ Ratio on CLG

Usually, one or more than one inert supporter is added to the oxygen carrier particles aiming to enhance the ionic–electronic conductivity and mechanical strength of the oxygen carrier particles. ZrO₂ was used as a binder and supporter to improve the performance of the NiFe₂O₄ OC. As shown in Figure 5, the carbon conversion and H₂ and CO production increased and then decreased as the proportion of NiFe₂O₄ increased. This is because NiFe₂O₄ provides lattice oxygen in the reaction to promote the reaction of bituminite. Too little NiFe₂O₄ was insufficient to provide the required lattice oxygen to react completely with the bituminite. Meanwhile, as an inert component, ZrO₂ can improve the reaction activity of the oxygen carrier, increasing the dispersion of the OC particles. ZrO₂ has a good modifying effect on the OC, and adding a certain amount of ZrO₂ will help the whole reaction system to proceed better. The addition of the NiFe₂O₄-to-ZrO₂ ratio of 7:3 was chosen as the best addition ratio.

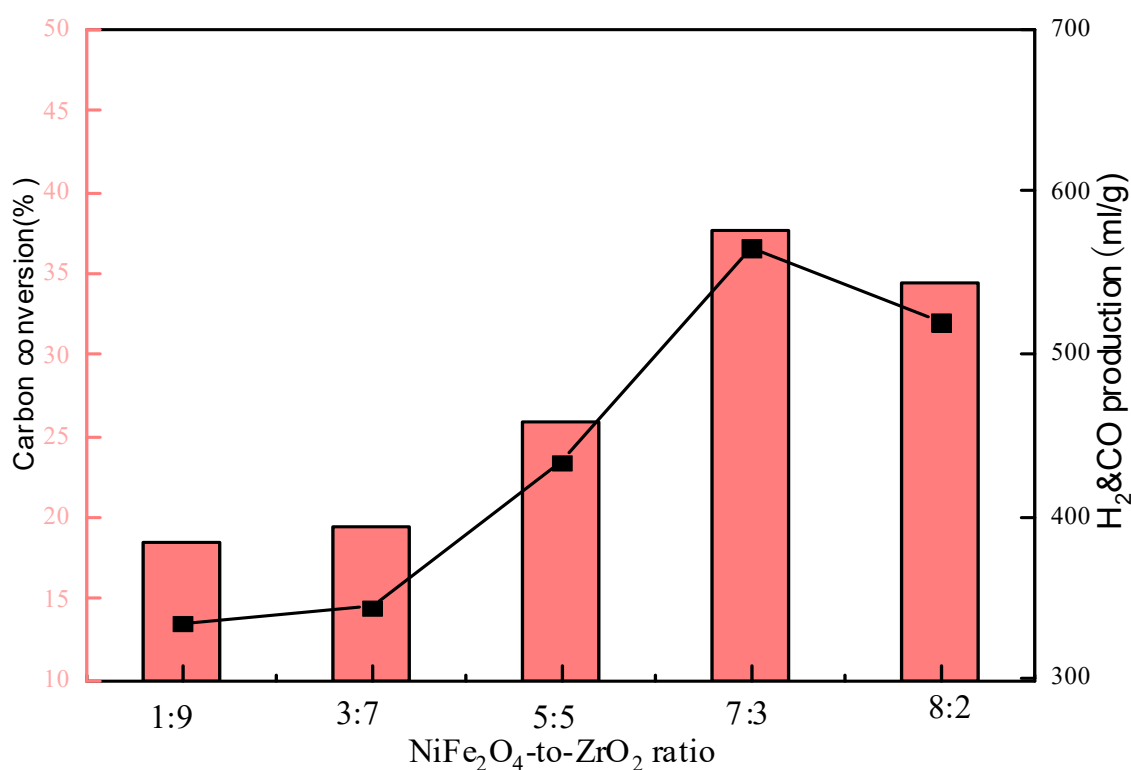


Figure 5. Effect of NiFe₂O₄-to-ZrO₂ ratio on CLG.

3.4. Effect of Alkali Metals Addition on CLG

The addition of alkali metals can also provide a significant modification in the oxygen carrier [48], and the synergistic effect between metals can largely improve the catalytic performance of the oxygen carrier.

The oxygen carrier for this experiment was a mixture of 1.63 g of NiFe₂O₄ and 0.7 g of ZrO₂. Different qualities of alkali lignin ash and K₂CO₃ reagent were selected as the sources of alkali metal in the present work. As shown in Figure 6, the carbon conversion increased from about 37% without alkali metals addition to a maximum of 80.6%, and the H₂ and CO production also increased from about 600 mL/g to about 1200 mL/g and reached its highest effect at the addition of 0.7 g alkali metal. The alkali metals promotion effect is mainly because the alkali metals modification weakens the strength of Fe–O bonds in oxygen carriers so that the oxygen carrier’s lattice oxygen can be better released, providing more lattice oxygen to participate in the reaction [48]. Meanwhile, it can reduce the activation energy of semi-coke gasification, so the oxygen carrier can better play a catalytic role. Alkali metals also have a certain catalytic ability, thus promoting the oxidative cracking of

bituminite coal volatile fraction and tar. Alkali lignin ash has a more pronounced modifying effect on oxygen carriers than K_2CO_3 . Alkali lignin ash was not effectively utilized and was discarded in large quantities, and it can be made into alkali lignin ash to realize its utilization value by co-gasification reaction with coal, so alkali lignin ash was selected as an additive. However, the reaction performance decreased instead when 0.9 g of alkali metals were added in, the promotion effect on the oxygen carrier was no longer obvious, and the sintering of the oxygen carrier was also found by the SEM. A total of 0.7 g of alkali lignin ash addition was an optimal choice to compound the conventional addition standard.

3.5. Effect of Steam Addition on CLG

The effects of varying the steam addition upon the gas composition, the CO and H_2 production, and the carbon conversion are shown in Figure 7. The results show that the addition of steam had an obvious effect on the production of H_2 . When the steam flow rate increased to 0.08 mL/min, the CO and H_2 production reached the maximum value of 2028 mL/g (about three times higher than the blank experiment without oxygen carriers). Meanwhile, carbon conversion was significantly improved. The maximum carbon conversion rate reached 94.64%, and the syngas selectivity at this point was 86.23%. The increase in carbon conversion and syngas production is due to the addition of steam enhanced the gasification process and promoted the steam reforming reaction in the reaction system ($H_2O + C \rightarrow H_2 + CO/H_2O + Tar \rightarrow H_2 + CO$). When adequate steam was added, the syngas CO production declined instead because the reaction ($H_2O + CO \rightarrow CO_2 + H_2$) was promoted, resulting in the production of useless CO_2 .

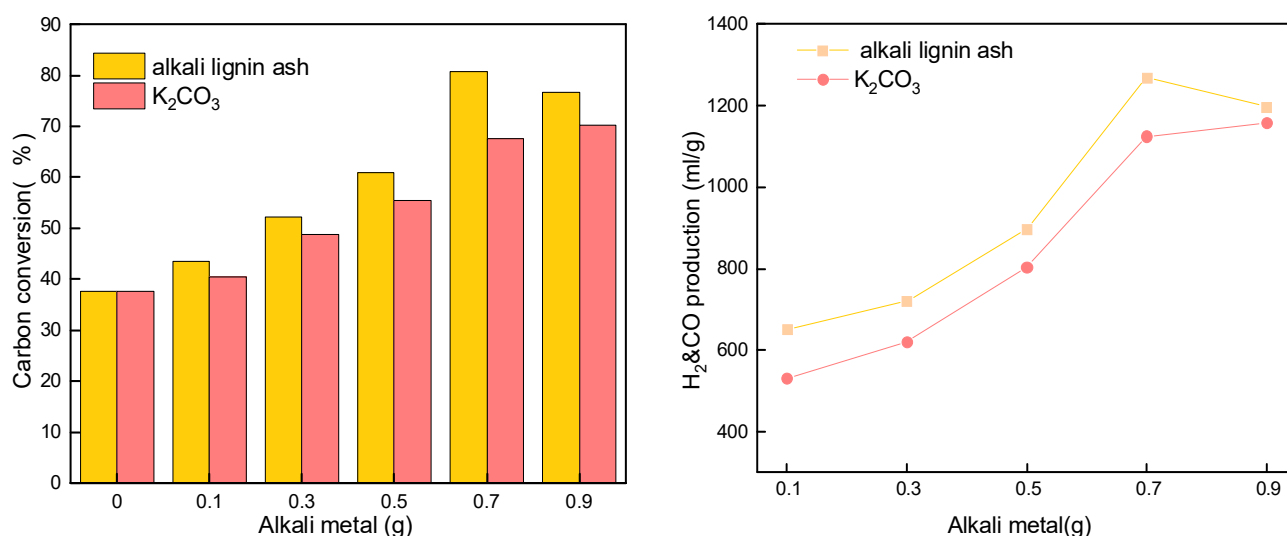


Figure 6. Effect of alkali metal addition on CLG.

However, the addition of excess steam may cause steam saturation on the surface of the oxygen carrier [49,50] and prevent the release of lattice oxygen from the lattice of the oxygen carrier so that the oxygen carrier does not play its role and also sintering of the oxygen carrier, which is not conducive to its participation in the cycle reaction. It will also generate useless CO_2 by water gas conversion reaction with CO. Meanwhile, it will also react with the oxygen carrier in the reduced state, so it is not advisable to add in excess. Combined with all standards, when under the experimental situation with 0.08 mL/min of steam added, the indicators reach a high level.

3.6. Long-Term Redox CLG

In order to demonstrate the good cycling performance of the oxygen carriers, 20 experiments with redox reactions were carried out. As shown in Figure 8, during 20 cycles, the carbon conversion was stable at about 90%, and the syngas selectivity was

maintained above 80%. In the first five redox experiments, the carbon conversion remained at a high level, while the carbon conversion showed a slight decrease from 5 to 10 cycles and a slightly increasing decrease trend from 10 to 15 cycles. However, the carbon conversion stabilized and showed a small increasing trend after 15 cycles.

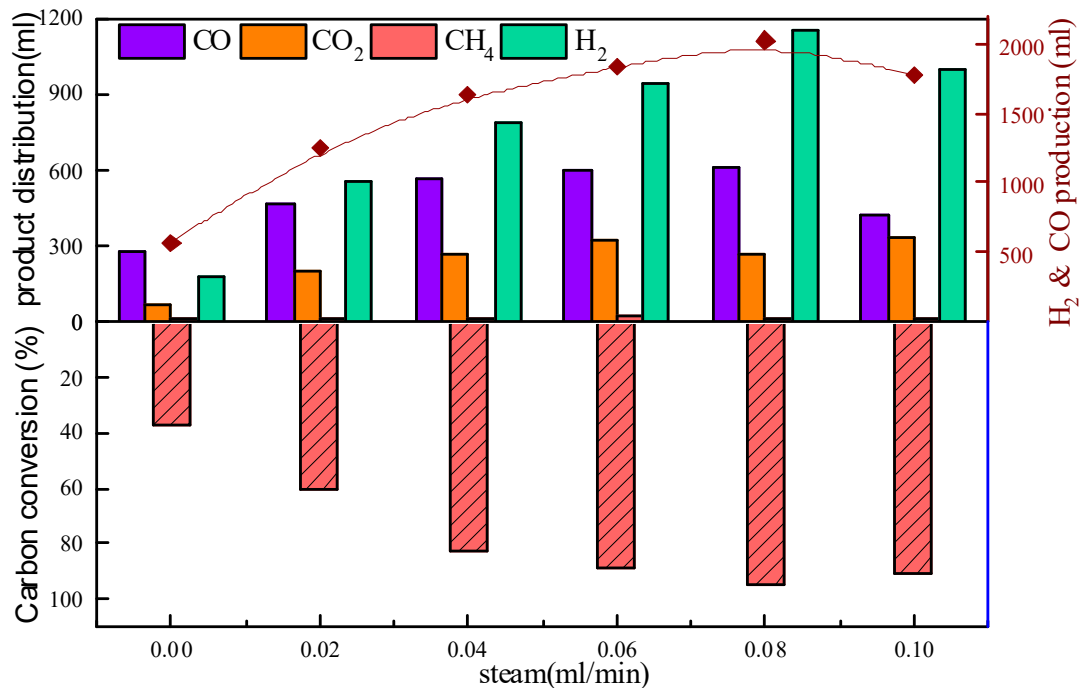


Figure 7. Effect of steam addition on CLG.

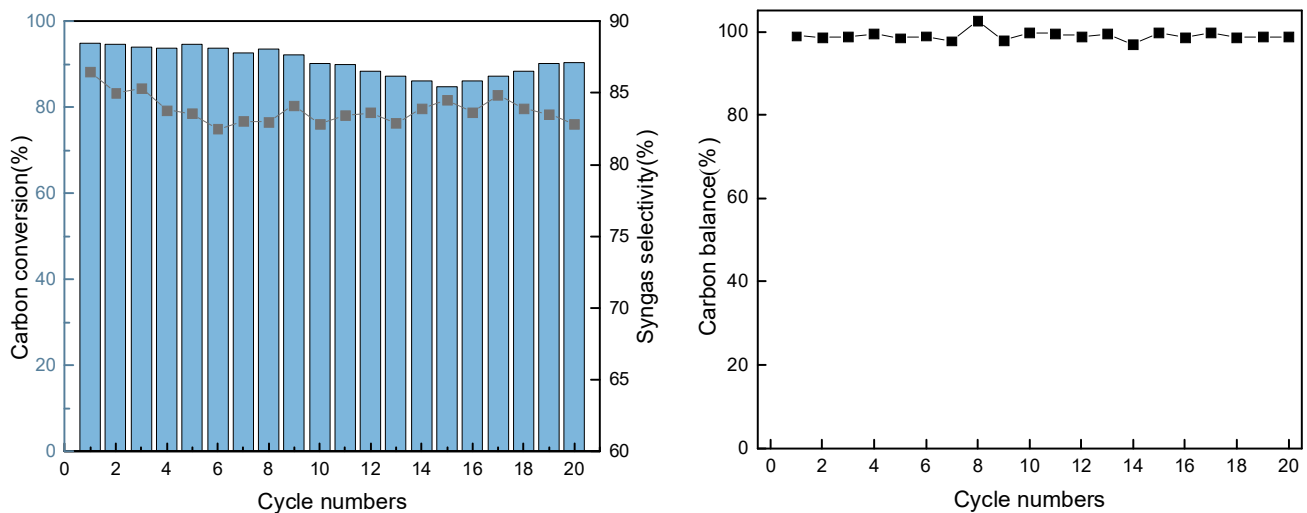


Figure 8. Results of the cyclic experiment.

The main reason for the previous decrease is that as the reaction proceeds, the phase of the oxygen carrier changes, and part of NiFe₂O₄ is not entirely oxidized and gradually exists in the form of Fe₂O₃ and NiO, so the reaction performance decreases, which is reflected in the XRD results. Another main reason is the sintering and agglomeration of oxygen carriers and the particle size increase during the cycling process, inhibiting the entry of gas molecules and leading to a decrease in performance, which is reflected in the SEM and TEM results. However, as the cycle proceeds, the coal ash gradually accumulates in the reactor, which causes the average residence time of the gas to be prolonged and the reaction

to be adequate. Meanwhile, coal ash has a certain oxidation activity, and increasingly alkali metals, especially a large amount of Ca, are enriched on the surface as the reaction proceeds, which is reflected in the TEM-mapping results. Ca has a certain catalytic ability, thus promoting the oxidative cracking of bituminite coal volatile fraction and tar, so the carbon conversion showed a small increase after 15 cycles. Coal ash possesses certain redox properties, while alkali metals can also promote the catalytic conversion of volatile and tar, which can compensate for the effect of oxygen carriers due to decreased activity. In addition, the carbon balance between 97% and 102% also indicates that most of the carbon is converted to carbon-containing gases, including CO and CO₂. Experiments show that the Ni₂FeO₄ oxygen carrier addition with ZrO₂ can be well applied to the CLG of Ningxia bituminite coal to prepare high-quality syngas with good cyclic reaction performance.

3.7. XRD Analysis

In order to study the physical phase changes in the oxygen carriers during the cycling process, XRD analysis was performed on the oxygen carriers of fresh, after reduction, 1 cycle, and 20 cycles. As shown in Figure 9, the main components of the fresh oxygen carrier are NiFe₂O₄ and ZrO₂. After the reduction, Ni²⁺ in the raw material is mainly reduced to Ni, Fe³⁺ is only partially reduced to Fe and FeO, and most of it is reduced to Fe₃O₄. The lattice oxygen of the oxygen carrier is mostly released in the reduction process. The main components in the oxygen carrier after one cycle remained the same as NiFe₂O₄ and ZrO₂. The peak of NiFe₂O₄ in the oxygen carrier became slightly smaller after one cycle. After 20 cycles, some of the NiFe₂O₄ was not reduced to its initial form. It existed in the form of the oxides of Fe, and part of Ni existed in the form of NiO, which is one of the main reasons for the slight decrease in the performance of the OC after multiple redox cycles. Meanwhile, a new phase of Ca₂Fe₂O₅ was formed after 20 cycles. However, the remaining NiFe₂O₄ produced in the OC after 20 cycles allows the OC to maintain a consistently good reaction performance in bituminite CLG.

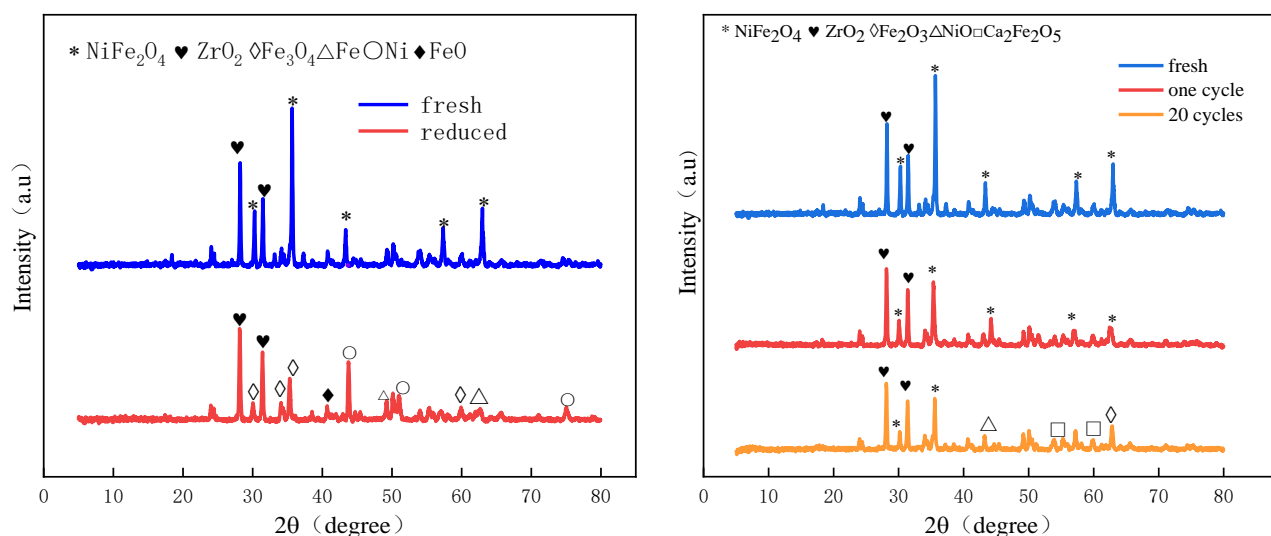


Figure 9. XRD patterns of fresh, reduced, 1 cycle, and 20 cycles.

3.8. SEM Analysis

To further investigate the surface morphology and structural changes in oxygen carriers after cycling, SEM characterization of fresh carriers fresh oxygen carrier, 5 cycles, and 20 cycles were performed. As shown in Figure 10, the fresh OC has a dense structure with a smooth and bright surface and possesses a large number of pore structures, thus having good reactivity in the gasification reaction. After five cycles, the particle size increases, but the surface remains smooth, and there is no obvious sintering. However, after 20 cycles, slight sintering and agglomeration appear, which explains the slight decrease in

the reactivity of the oxygen carrier. The surface remains smooth and flat, and the porous structure is still good, which is one of the key factors in maintaining the good CLG cycling performance of the oxygen carrier.

SEM results of different added masses of alkali lignin ash and K_2CO_3 were tested to further investigate the effect of alkali metal addition on the surface morphology of the oxygen carrier. As shown in Figure 11, the surface morphological structure of the oxygen carrier after the reaction of adding 0.1 g alkali lignin ash did not change much compared with the original oxygen carrier, but the addition of 0.1 g K_2CO_3 showed a slight agglomeration and sintering phenomenon. The addition of 0.5 g of alkali lignin ash showed an obvious porous structure with larger particle size and no agglomeration and sintering. The addition of 0.5 g of K_2CO_3 showed obvious agglomeration and sintering, which is one of the reasons why the improvement in chemical looping gasification performance by alkali lignin ash is better than the addition of K_2CO_3 . When adding up to 0.9 g of K_2CO_3 and alkali lignin ash, the oxygen carrier showed significant agglomeration and sintering, which is one of the main reasons for the decrease in oxygen carrier performance. On the one hand, the addition of alkali metals will have a catalytic effect on the pyrolysis and gasification process of bituminite, thus improving its utilization efficiency. On the other hand, the addition of excessive alkali metal will cause severe sintering on the surface of the oxygen carrier, destroying the porous structure of the OC and blocking the pores, thus leading to a decrease in the reaction performance of the OC.

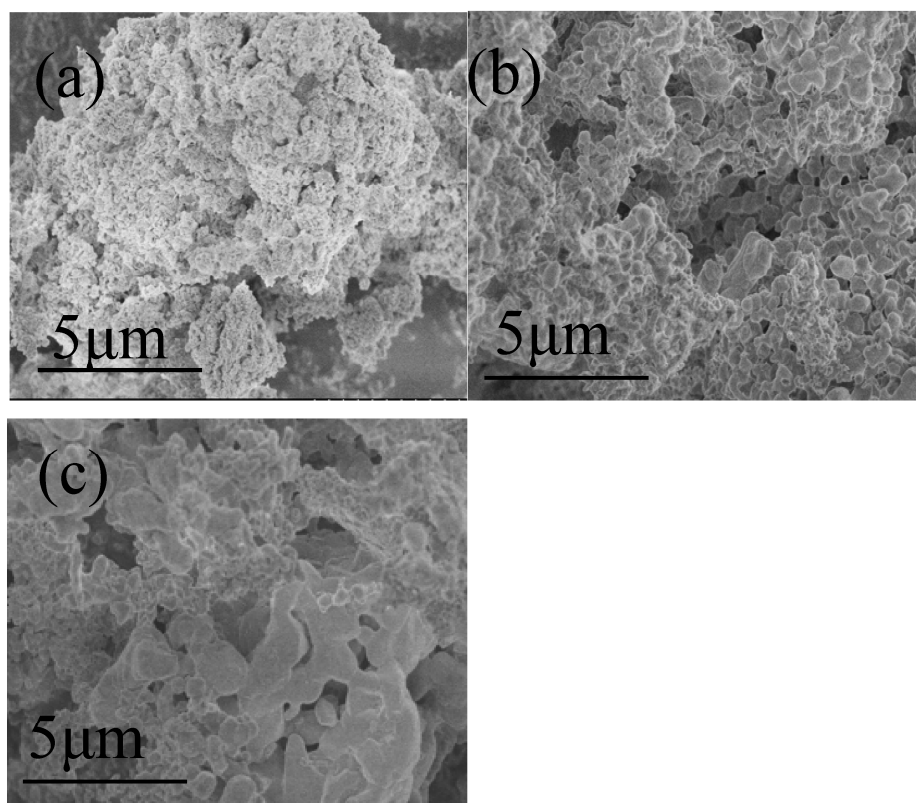


Figure 10. SEM photographs of the oxygen carriers: (a) fresh, (b) after 5 cycles, (c) after 20 cycles.

3.9. TEM Analysis

TEM images of the sample after 1 cycle, 5 cycles, and 20 cycles are shown in Figure 12a, Figure 12b, and Figure 12c, respectively. The particle size after one cycle is around 150–200 nm. After five cycles, the particle size of the OC sample shows a slight increase to around 200–250 nm. With the increase in cycles, the sample gradually sintered, causing an increase in the particle size. After 20 redox cycles, the particle size of the OC sample is more than 400 nm. The large particle size inhibits the gas molecules from penetrating

into the interior of the OC, resulting in the reduction in redox reaction rate, and reduced reaction performance of oxygen carriers with bituminite.

As shown in Figure 13, Fe and Ni elements are uniformly distributed in the fresh oxygen carrier particles. After 20 cycles, there is still a large amount of Fe on the surface, but the Ni on the surface massive decreases, which shows that as the reaction proceeds, the oxide of Ni and NiFe_2O_4 is gradually encapsulated by the oxide of Fe. Meanwhile, the element Ca from the long-term cycle of bituminite accumulation starts to appear on the surface in large quantities, corresponding to the formation of the $\text{Ca}_2\text{Fe}_2\text{O}_5$ phase observed in XRD. As an alkaline earth metal, Ca promotes the reaction performance of oxygen carriers to some extent and facilitates the gasification reaction, but gradually formed $\text{Ca}_2\text{Fe}_2\text{O}_5$ will reduce the reaction activity of oxygen carriers, thus inhibiting the redox reaction.

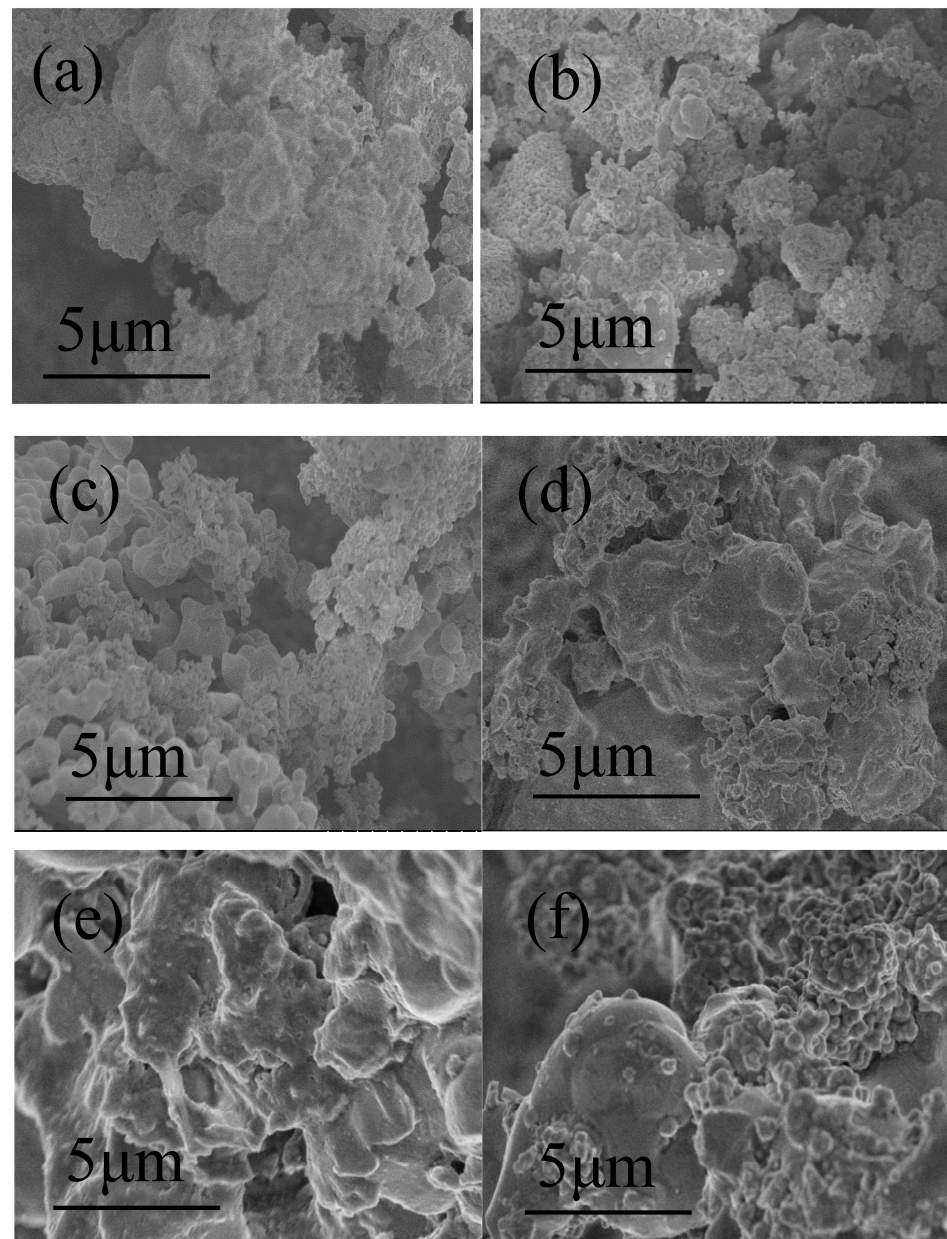


Figure 11. SEM photographs of the oxygen carrier with different alkali metal additions: (a) 0.1 g alkali lignin ash, (b) 0.1 g K_2CO_3 , (c) 0.5 g alkali lignin ash, (d) 0.5 g K_2CO_3 , (e) 0.9 g alkali lignin ash, (f) 0.9 g K_2CO_3 .

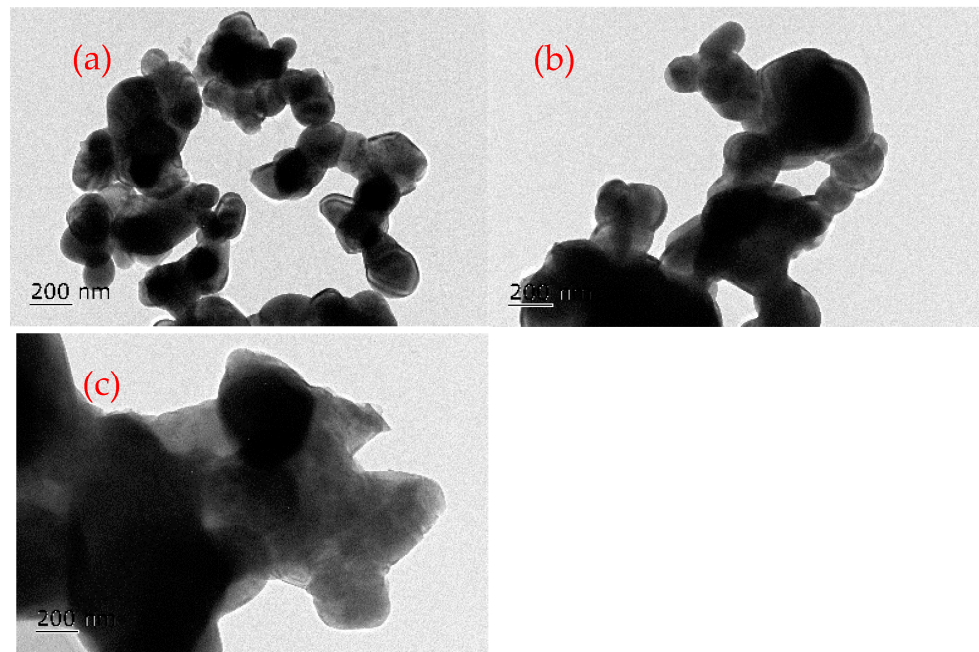
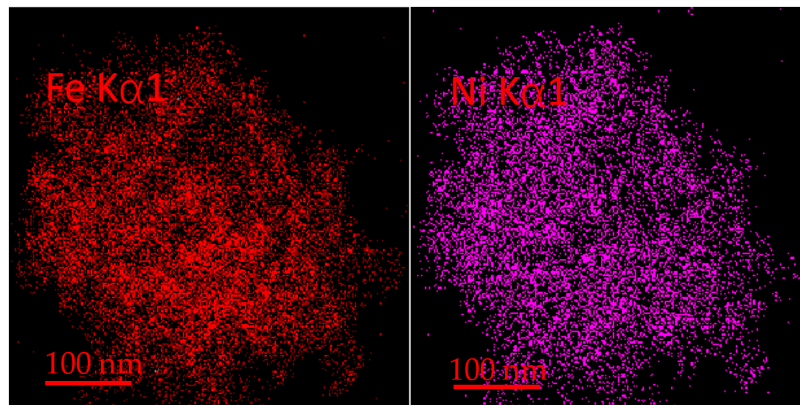
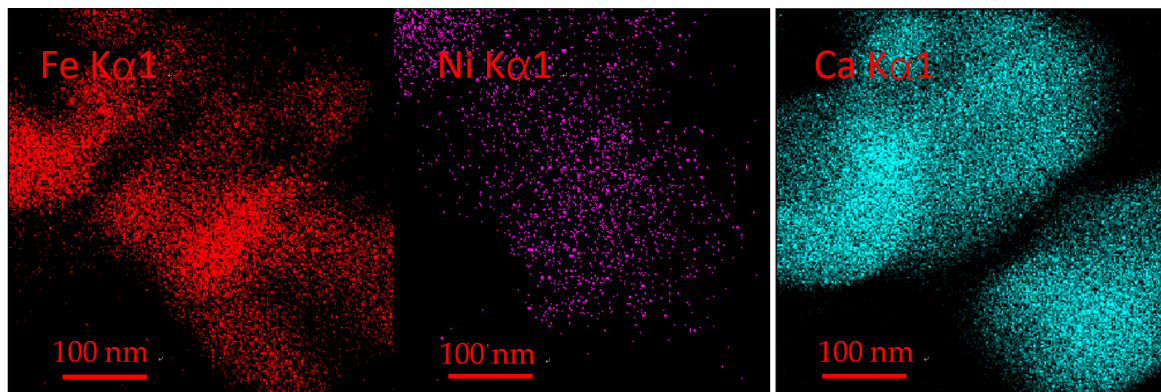


Figure 12. TEM photographs of the OC after different cycle numbers: (a) after 1 cycle, (b) after 5 cycles, (c) after 20 cycles.



(a)



(b)

Figure 13. (a) EDS of fresh OC. (b) EDS of OC after 20 cycles.

4. Conclusions

In this work, NiFe_2O_4 was used as the oxygen carrier for CLG of bituminite to produce high-quality syngas. The effects of temperature, O/B, ZrO_2 , steam, and alkali metal addition were systematically investigated in a fixed-bed reactor. The results show that the elevated temperature and adding a fraction of steam facilitate the gasification reaction. Adding an appropriate amount of ZrO_2 into the NiFe_2O_4 and modification with alkali metal can enhance the performance of the oxygen carrier. A carbon conversion of 95% and a syngas (CO and H_2) selectivity of 86% were obtained under the optimized reaction conditions of 950 °C, an oxygen-carrier-to-bituminite (O/B) ratio of 7:3, a $\text{NiFe}_2\text{O}_4/\text{ZrO}_2$ ratio of 7:3, and a steam rate of 0.08 mL/min. Modification of the NiFe_2O_4 by doping alkali metal can significantly facilitate the CLG process. Alkali lignin ash has a more pronounced modifying effect on oxygen carriers than K_2CO_3 , and the best modification effect is achieved at 0.7 g addition.

The changes in the various stages of the oxygen carrier and its role in the reaction process are also analyzed from a microscopic perspective. The NiFe_2O_4 oxygen carrier underwent a gradual reduction in $\text{Ni}^{2+} \rightarrow \text{Ni}$ and $\text{Fe}^{3+} \rightarrow \text{Fe}^{8/3+} \rightarrow \text{Fe}^{2+} \rightarrow \text{Fe}$ processes during the gasification reaction phase. Meanwhile, 20 cycles of experiments are carried out, and the oxygen carrier consistently maintains good reactivity and thermal stability during the cycles. The surface remains smooth and flat, and the porous structure remains good after 20 cycles. It is proved that the NiFe_2O_4 oxygen carrier addition with ZrO_2 has the advantages of lattice oxygen transfer capability, good reaction performance, good mechanical stability, excellent catalytic cracking tar performance, and cyclic sustainability. This work laid the theoretical foundation for the clean and efficient use of bituminite.

Author Contributions: Conceptualization, M.Y.; methodology, G.W.; software, M.Y.; validation, M.Y. and G.W.; formal analysis, G.W. and F.H.; investigation, D.S. and Y.L.; resources, M.Y.; data curation, M.Y.; writing—original draft preparation, M.Y.; writing—review and editing, G.W. and F.H.; visualization, G.W.; supervision, G.W. and F.H.; project administration, D.S. and J.C.; funding acquisition, G.W. and F.H. All authors have read and agreed to the published version of the manuscript.

Funding: This research was funded by the National Natural Science Foundation of China (22179027, 52276191, 51976226) and the Guangxi Natural Science Foundation (2021GXNSFAA075036).

Data Availability Statement: Not applicable.

Acknowledgments: The authors gratefully acknowledge the National Natural Science Foundation of China (22179027, 52276191, 51976226) and the Guangxi Natural Science Foundation (2021GXNSFAA075036).

Conflicts of Interest: The authors declare no conflict of interest.

References

1. Li, X.-H.; Li, H.-J.; Wang, R.-Q.; Feng, J.; Li, W.-Y. Acid pretreatment effect on oxygen migration during lignite pyrolysis. *Fuel* **2020**, *262*, 116650. [[CrossRef](#)]
2. Liu, G.; Zhang, Y.; Zhou, A.; Wang, J.; Cai, J.; Dang, Y. A Comparative Study on the Performance of Direct Carbon Solid Oxide Fuel Cells Powered with Different Rank Coals. *Energy Fuels* **2021**, *35*, 6835–6844. [[CrossRef](#)]
3. Wang, G.; Xu, Y.; Ren, H. Intelligent and ecological coal mining as well as clean utilization technology in China: Review and prospects. *Int. J. Min. Sci. Technol.* **2019**, *29*, 161–169. [[CrossRef](#)]
4. Zhao, Y.; Cui, Z.; Wu, L.; Gao, W. The green behavioral effect of clean coal technology on China's power generation industry. *Sci. Total Environ.* **2019**, *675*, 286–294. [[CrossRef](#)]
5. Richter, H.J.; Knoche, K.F. Reversibility of Combustion Processes. In *Efficiency and Costing*; ACS Publications: Washington, DC, USA, 1983; pp. 71–85. [[CrossRef](#)]
6. Cormos, A.-M.; Chisalita, D.-A. Assessment of chemical looping combustion process by dynamic simulation. *Comput. Aided Chem. Eng.* **2016**, *38*, 271–276. [[CrossRef](#)]
7. Czakiert, T.; Krzywanski, J.; Zylka, A.; Nowak, W. Chemical Looping Combustion: A Brief Overview. *Energies* **2022**, *15*, 1563. [[CrossRef](#)]
8. Noorman, S.; Annaland, M.V.S.; Kuipers, J. Experimental validation of packed bed chemical-looping combustion. *Chem. Eng. Sci.* **2010**, *65*, 92–97. [[CrossRef](#)]

9. Di Giuliano, A.; Capone, S.; Anatone, M.; Gallucci, K. Chemical Looping Combustion and Gasification: A Review and a Focus on European Research Projects. *Ind. Eng. Chem. Res.* **2022**, *61*, 14403–14432. [[CrossRef](#)]
10. Fan, L.; Li, F.; Ramkumar, S. Utilization of chemical looping strategy in coal gasification processes. *Particuology* **2008**, *6*, 131–142. [[CrossRef](#)]
11. Zhao, K.; Fang, X.; Huang, Z.; Wei, G.; Zheng, A.; Zhao, Z. Hydrogen-rich syngas production from chemical looping gasification of lignite by using NiFe₂O₄ and CuFe₂O₄ as oxygen carriers. *Fuel* **2021**, *303*, 121269. [[CrossRef](#)]
12. De Diego, L.F.; Garcá-Labiano, F.; Gayán, P.; Celaya, J.; Palacios, J.M.; Adánez, J. Operation of a 10 kW_{th} chemical-looping combustor during 200 h with a CuO–Al₂O₃ oxygen carrier. *Fuel* **2007**, *86*, 1036–1045. [[CrossRef](#)]
13. Marx, F.; Dieringer, P.; Ströhle, J.; Epple, B. Design of a 1 MW_{th} Pilot Plant for Chemical Looping Gasification of Biogenic Residues. *Energies* **2021**, *14*, 2581. [[CrossRef](#)]
14. Thon, A.; Kramp, M.; Hartge, E.-U.; Heinrich, S.; Werther, J. Operational experience with a system of coupled fluidized beds for chemical looping combustion of solid fuels using ilmenite as oxygen carrier. *Appl. Energy* **2014**, *118*, 309–317. [[CrossRef](#)]
15. Li, F.; Zeng, L.; Velazquez-Vargas, L.G.; Yoscovits, Z.; Fan, L.-S. Syngas chemical looping gasification process: Bench-scale studies and reactor simulations. *AIChE J.* **2010**, *56*, 2186–2199. [[CrossRef](#)]
16. Sarafraz, M.; Jafarian, M.; Arjomandi, M.; Nathan, G. The thermo-chemical potential liquid chemical looping gasification with bismuth oxide. *Int. J. Hydrogen Energy* **2019**, *44*, 8038–8050. [[CrossRef](#)]
17. Guan, Y.; Liu, Y.; Lin, X.; Wang, B.; Lyu, Q. Research Progress and Perspectives of Solid Fuels Chemical Looping Reaction with Fe-Based Oxygen Carriers. *Energy Fuels* **2022**, *36*, 13956–13984. [[CrossRef](#)]
18. Mendiara, T.; Pérez, R.; Abad, A.; de Diego, L.F.; García-Labiano, F.; Gayán, P.; Adánez, J. Low-Cost Fe-Based Oxygen Carrier Materials for the iG-CLC Process with Coal. 1. *Ind. Eng. Chem. Res.* **2012**, *51*, 16216–16229. [[CrossRef](#)]
19. Yuan, N.; Bai, H.; An, M.; Zhang, J.; Hu, X.; Guo, Q. Modulation of Fe-based oxygen carriers by low concentration doping of Cu in chemical looping process: Reactivity and mechanism based on experiments combined with DFT calculations. *Powder Technol.* **2021**, *388*, 474–484. [[CrossRef](#)]
20. Feng, Y.; Guo, X. Study of reaction mechanism of methane conversion over Ni-based oxygen carrier in chemical looping reforming. *Fuel* **2017**, *210*, 866–872. [[CrossRef](#)]
21. Liu, C.; Chen, D.; Tang, Q.; Abuelgasim, S.; Xu, C.; Luo, J.; Zhao, Z.; Abdalazeez, A. Hydrogen-rich syngas production from straw char by chemical looping gasification: The synergistic effect of Mn and Fe on Ni-based spinel structure as oxygen carrier. *Fuel* **2023**, *334*, 126803. [[CrossRef](#)]
22. Rasi, N.M.; Karcz, A.; Ponnurangam, S.; Mahinpey, N. Insight into MgO-supported NiO reactivity from atomic-scale electronegativity for oxygen carrier design and catalyst production applications. *Catalysis Today* **2022**, *404*, 244–252. [[CrossRef](#)]
23. Gayán, P.; Forero, C.R.; Abad, A.; de Diego, L.F.; García-Labiano, F.; Adánez, J. Effect of Support on the Behavior of Cu-Based Oxygen Carriers during Long-Term CLC Operation at Temperatures above 1073 K. *Energy Fuels* **2011**, *25*, 1316–1326. [[CrossRef](#)]
24. Wang, S.; Luo, M.; Wang, G.; Wang, L.; Lv, M. Analysis of Reactivity of a CuO-Based Oxygen Carrier for Chemical Looping Combustion of Coal. *Energy Fuels* **2012**, *26*, 3275–3283. [[CrossRef](#)]
25. Zhao, H.; Guo, L.; Zou, X. Chemical-looping auto-thermal reforming of biomass using Cu-based oxygen carrier. *Appl. Energy* **2015**, *157*, 408–415. [[CrossRef](#)]
26. Cao, Y.; He, B.; Yan, L. Process simulation of a dual fluidized bed chemical looping air separation with Mn-based oxygen carrier. *Energy Convers. Manag.* **2019**, *196*, 286–295. [[CrossRef](#)]
27. Jacobs, M.; van der Kolk, T.; Albertsen, K.; Mattisson, T.; Lyngfelt, A.; Snijders, F. Synthesis and upscaling of perovskite Mn-based oxygen carrier by industrial spray drying route. *Int. J. Greenh. Gas Control* **2018**, *70*, 68–75. [[CrossRef](#)]
28. Bi, W.; Chen, T.; Zhao, R.; Wang, Z.; Wu, J.; Wu, J. Characteristics of a CaSO₄ oxygen carrier for chemical-looping combustion: Reaction with polyvinylchloride pyrolysis gases in a two-stage reactor. *RSC Adv.* **2015**, *5*, 34913–34920. [[CrossRef](#)]
29. Liu, S.; Lee, D.; Liu, M.; Li, L.; Yan, R. Selection and Application of Binders for CaSO₄ Oxygen Carrier in Chemical-Looping Combustion. *Energy Fuels* **2010**, *24*, 6675–6681. [[CrossRef](#)]
30. Liu, Y.; Gao, M.; Zhang, X.; Hu, X.; Guo, Q. Characteristics of a CaSO₄ composite oxygen carrier supported with an active material for *in situ* gasification chemical looping combustion of coal. *RSC Adv.* **2018**, *8*, 23372–23381. [[CrossRef](#)]
31. Wei, G.; Wang, H.; Zhao, W.; Huang, Z.; Yi, Q.; He, F.; Zhao, K.; Zheng, A.; Meng, J.; Deng, Z.; et al. Synthesis gas production from chemical looping gasification of lignite by using hematite as oxygen carrier. *Energy Convers. Manag.* **2019**, *185*, 774–782. [[CrossRef](#)]
32. Chen, Z.; Liao, Y.; Liu, G.; Mo, F.; Ma, X. Application of Mn–Fe Composite Oxides Loaded on Alumina as Oxygen Carrier for Chemical Looping Gasification. *Waste Biomass-Valorization* **2019**, *11*, 6395–6409. [[CrossRef](#)]
33. Maya, J.C.; Chejne, F.; Bhatia, S.K. Effect of sintering on the reactivity of copper-based oxygen carriers synthesized by impregnation. *Chem. Eng. Sci.* **2017**, *162*, 131–140. [[CrossRef](#)]
34. Sikarwar, S.S.; Vooradi, R.; Patnaikuni, V.S.; Kakunuri, M.; Surywanshi, G.D. A novel thermally stable Fe₂O₃/Al₂O₃ nanofiber-based oxygen carrier for chemical-looping combustion. *Chem. Papers* **2022**, *76*, 3987–3993. [[CrossRef](#)]
35. Wang, K.; Yu, Q.; Wang, Q.; Hua, J.; Peng, R. Oxygen Uncoupling Property and Kinetics of a Copper Manganese Composite Oxygen Carrier in a Packed-Bed Reactor. *Energy Fuels* **2020**, *34*, 6158–6167. [[CrossRef](#)]
36. Song, T.; Shen, T.; Shen, L.; Xiao, J.; Gu, H.; Zhang, S. Evaluation of hematite oxygen carrier in chemical-looping combustion of coal. *Fuel* **2013**, *104*, 244–252. [[CrossRef](#)]

37. Zheng, A.; Fan, Y.; Wei, G.; Zhao, K.; Huang, Z.; Zhao, Z.; Li, H. Chemical Looping Gasification of Torrefied Biomass Using NiFe_2O_4 as an Oxygen Carrier for Syngas Production and Tar Removal. *Energy Fuels* **2020**, *34*, 6008–6019. [[CrossRef](#)]
38. Huang, Z.; Deng, Z.; Chen, D.; He, F.; Liu, S.; Zhao, K.; Wei, G.; Zheng, A.; Zhao, Z.; Li, H. Thermodynamic analysis and kinetic investigations on biomass char chemical looping gasification using Fe-Ni bimetallic oxygen carrier. *Energy* **2017**, *141*, 1836–1844. [[CrossRef](#)]
39. Lyngfelt, A.; Leckner, B.; Mattisson, T. A fluidized-bed combustion process with inherent CO_2 separation; application of chemical-looping combustion. *Chem. Eng. Sci.* **2001**, *56*, 3101–3113. [[CrossRef](#)]
40. Wei, G.; He, F.; Huang, Z.; Zheng, A.; Zhao, K.; Li, H. Continuous Operation of a 10 kW(th) Chemical Looping Integrated Fluidized Bed Reactor for Gasifying Biomass Using an Iron-Based Oxygen Carrier. *Energy Fuels* **2015**, *29*, 233–241. [[CrossRef](#)]
41. Li, K.; Wang, H.; Wei, Y.; Yan, D. Direct conversion of methane to synthesis gas using lattice oxygen of $\text{CeO}_2\text{-Fe}_2\text{O}_3$ complex oxides. *Chem. Eng. J.* **2010**, *156*, 512–518. [[CrossRef](#)]
42. Jiang, L.; Hu, S.; Wang, Y.; Su, S.; Sun, L.; Xu, B.; He, L.; Xiang, J. Catalytic effects of inherent alkali and alkaline earth metallic species on steam gasification of biomass. *Int. J. Hydrogen Energy* **2015**, *40*, 15460–15469. [[CrossRef](#)]
43. Lv, D.; Xu, M.; Liu, X.; Zhan, Z.; Li, Z.; Yao, H. Effect of cellulose, lignin, alkali and alkaline earth metallic species on biomass pyrolysis and gasification. *Fuel Process. Technol.* **2010**, *91*, 903–909. [[CrossRef](#)]
44. Ge, H.; Shen, L.; Gu, H.; Jiang, S. Effect of co-precipitation and impregnation on K-decorated $\text{Fe}_2\text{O}_3/\text{Al}_2\text{O}_3$ oxygen carrier in Chemical Looping Combustion of bituminous coal. *Chem. Eng. J.* **2015**, *262*, 1065–1076. [[CrossRef](#)]
45. Zhao, H.; Mei, D.; Ma, J.; Zheng, C. Comparison of preparation methods for iron-alumina oxygen carrier and its reduction kinetics with hydrogen in chemical looping combustion. *Asia-Pacific J. Chem. Eng.* **2014**, *9*, 610–622. [[CrossRef](#)]
46. Ma, Z.; Zhang, S.; Xiao, R. Insights into the relationship between microstructural evolution and deactivation of Al_2O_3 supported Fe_2O_3 oxygen carrier in chemical looping combustion. *Energy Convers. Manag.* **2019**, *188*, 429–437. [[CrossRef](#)]
47. Shen, L.; Wu, J.; Gao, Z.; Xiao, J. Reactivity deterioration of $\text{NiO}/\text{Al}_2\text{O}_3$ oxygen carrier for chemical looping combustion of coal in a 10 kWth reactor. *Combust. Flame* **2009**, *156*, 1377–1385. [[CrossRef](#)]
48. Yu, Z.; Li, C.; Fang, Y.; Huang, J.; Wang, Z. Reduction Rate Enhancements for Coal Direct Chemical Looping Combustion with an Iron Oxide Oxygen Carrier. *Energy Fuels* **2012**, *26*, 2505–2511. [[CrossRef](#)]
49. Siriwardane, R.; Riley, J.; Tian, H.; Richards, G. Chemical looping coal gasification with calcium ferrite and barium ferrite via solid–solid reactions. *Appl. Energy* **2016**, *165*, 952–966. [[CrossRef](#)]
50. Wu, Y.; Liao, Y.; Liu, G.; Ma, X. Syngas production by chemical looping gasification of biomass with steam and CaO additive. *Int. J. Hydrogen Energy* **2018**, *43*, 19375–19383. [[CrossRef](#)]

Disclaimer/Publisher’s Note: The statements, opinions and data contained in all publications are solely those of the individual author(s) and contributor(s) and not of MDPI and/or the editor(s). MDPI and/or the editor(s) disclaim responsibility for any injury to people or property resulting from any ideas, methods, instructions or products referred to in the content.